PCCP

Accepted Manuscript

ROYAL SOCIETY OF CHEMISTRY

www.rsc.org/pccp

Journal Name

ARTICLE

Mixtures of the 1-ethyl-3-methylimidazolium acetate ionic liquid with different inorganic salts: Insights into their interactions

Received 00th January 20xx,
Accepted 00th January 20xx

DOI: 10.1039/x0xx00000x

www.rsc.org/

Filipe S. Oliveira,[a] Eurico J. Cabrita,[b] Smilja Todorovic,[a] Carlos E. S. Bernardes,[c] José N. Canongia Lopes,[a,c] Jennifer L. Hodgson,[d] Douglas R. MacFarlane,[d] Luís P. N. Rebelo[a] and Isabel M. Marrucho*[a]

In this work, we explore the interactions between the ionic liquid 1-ethyl-3-methylimidazolim acetate and different inorganic salts belonging to two different cation families, those based on ammonium and others based on sodium. NMR and Raman spectroscopy are used to screen for changes in the molecular environment of the ions in the ionic liquid + inorganic salt mixtures as compared to pure ionic liquid. The ion self-diffusion coefficients are determined from NMR data, allowing the discussion of the ionicity values of the ionic liquid + inorganic salt mixtures calculated using different methods. Our data reveal that preferential interactions are established between the ionic liquid and ammonium-based salts, as opposed to sodium-based salts. Computational calculations show the formation of aggregates between the ionic liquid and the inorganic salt, which is consistent with the spectroscopic data, and indicate that the acetate anion of the ionic liquid establishes preferential interactions with the ammonium cation of the inorganic salts, leaving the imidazolium cation less engaged in the media.

Introduction

Ionic liquids (ILs) are low melting salts which possess a wide range of unique properties, often including negligible vapour pressure, large liquid range, highly specific and tunable solvent ability, that are responsible for the increased interest in this class of compounds in recent decades.[1, 2]

Although ILs are formally composed of discrete ions, these compounds form aggregates and clusters to some extent, as a result of their complex nature that emerges from the interplay between their Coulombic, hydrogen-bonding and dispersive (van der Waals and π–π) interactions. Furthermore, studies have shown that ILs can be nanostructured, i.e., composed of segregated polar and nonpolar domains on the nano scale, where the polar domain is composed of the high charge-density parts of both the cations and anions, while the apolar domain is typically constituted by the alkane-type moieties of the organic ions.[3] These different levels of structuring, even on relatively short timescales, can lower the ionic conductivity of the liquid since some of the ions are bound into neutral species. To quantify this effect, a quantity termed the "ionicity" has been defined. Ionicity describes the ratio of measured molar conductivity to that calculated through the Nernst-Einstein equation from measured diffusion coefficients. An alternative qualitative approach uses the Walden plot to estimate ionicity.[4-7]

Lately, Molecular Dynamics (MD) and Density Functional Theory (DFT) calculations have become powerful tools for the understanding of thermophysical properties and phase equilibria, contributing important insights into structure-property relationships of ILs. Brüssel et al.[8, 9], used *ab initio* MD calculations to study the binary mixture of the ILs based on the 1-ethyl-3-methylimidazolium cation combined with thiocyanate and chloride anions. These authors showed that while in the neat ILs the main anion–cation interaction takes place through the most acidic proton of the imidazolium ring (H2), this observation does not hold for their mixtures. Umebayashi et al.[10, 11] used Raman spectroscopy and *ab initio* calculations to study the solvation structure of the lithium ion (from lithium bis(trifluoromethylsulfonyl)amide salt, Li[NTf_2]) in three different ILs, two imidazolium-based (1-ethyl-3-methylimidazolium bis(trifluoromethylsulfonyl)amide and 1-butyl-3-methylimidazolium bis(trifluoromethylsulfonyl)amide) and one pyrrolidinium-based (N-butyl-N-methylpyrrolidinium bis(trifluoromethylsulfonyl)amide). The *ab initio* calculations showed that the lithium cation coordinated to the four oxygen atoms of the bidentate [NTf_2]$^-$ anion and that the IL cation played a key role in the stabilization of the complex formed by the lithium cation and [NTf_2]$^-$ anions. Tsuzuki et al.[12] studied

[a] Instituto de Tecnologia Química e Biológica António Xavier, Universidade Nova de Lisboa, Av. da República, 2780-157 Oeiras, Portugal. E-mail: imarrucho@itqb.unl.pt
[b] UCIBIO, REQUIMTE, Departamento de Química, Faculdade de Ciências e Tecnologia, Universidade Nova de Lisboa, P-2829516 Caparica, Portugal
[c] Centro de Química Estrutural, Instituto Superior Técnico, 1049-001 Lisboa, Portugal.
[d] School of Chemistry, Monash University, Clayton, 3800 VIC, Australia.

† Electronic Supplementary Information (ESI) available: ^{1}H NMR spectra and tables with the chemical shifts. Diffusion plots and table with experimental values. Tables and figures with DFT obtained data for the IL, ISs and clusters as well as all the different conformations screened. See DOI: 10.1039/x0xx00000x

the transport properties of the 1-ethyl-3-methylimidazolium bis(fluorosulfonyl)amide IL and its lithium salt mixtures and used *ab initio* calculations to infer the stabilization energies of the complexes formed between the different ions. The obtained results were compared with those of the 1-ethyl-3-methylimidazolium bis(trifluoromethylsulfonyl)amide IL and also its lithium salt mixture. In both cases the imidazolium and the lithium cations showed weaker electrostatic and induction interactions with the bis(fluorosulfonyl)amide anion than with the bis(trifluoromethylsulfonyl)amide anion, corroborating the lower viscosity of the system containing the first anion.

NMR spectroscopy offers the ability to study changes in an IL's supramolecular structure with solvation, enabling a closer insight into the molecular interactions *in situ*. In particular, nuclear Overhauser effect (NOE) techniques can be very useful in the study of solvation and preferential interactions of neat IL and IL mixtures.[13-16] The analysis of intermolecular NOEs in solution can reflect the mutual position of interacting species in terms of short range effects (d < 5Å) or, as proposed by Gabl et al.[17], be a consequence of long-range effects and interactions far beyond the first coordination shell. The combination of NOE data with MD simulations is therefore a powerful tool for the rationalization of the intricate network of interactions occurring in ILs at the nano-level.

In our recent work,[18] we reported thermophysical properties of mixtures of 1-ethyl-3-methylimidazolium acetate IL with several ammonium/sodium-based inorganic salts (ISs) and estimated their ionicity through the Walden plot approach. Different behaviours were observed upon the addition of different ISs; for instance, when sodium-based ISs were added the ionicity of the system decreased, while in ammonium-based ISs the opposite behaviour was found. In addition, when ammonium thiocyanate was added to the IL, the mixtures showed distinct behaviours when compared with the other ISs used. In this particular system, we observed that the conductivity increased, while the viscosity was almost constant upon the addition of IS, leading to the highest ionicity of the IL + IS systems studied.

As a follow up of our previous work, in the present study we explore the interactions that occur between the IL and IS in order to understand the increase in the ionicity caused by the addition of IS to the IL media. The IL used was the 1-ethyl-3-methylimidazolium acetate and the effect of the addition of six different ISs namely, ammonium acetate, ammonium chloride, ammonium thiocyanate, ammonium ethane sulfonate, sodium acetate and sodium thiocyanate, were studied. Spectroscopic methods, NMR and Raman, were used to probe the changes in the bulk IL as the IS concentration was increased; MD and DFT calculations complement and support the discussion of our spectroscopic findings. In addition, the ionicity calculated through different methods is discussed.

Experimental

Materials

The following six ISs were used in this work: ammonium acetate ($[NH_4][Ac]$), ammonium chloride ($[NH_4]Cl$), ammonium thiocyanate ($[NH_4][SCN]$), ammonium ethane sulfonate ($[NH_4][EtSO_3]$), sodium acetate (Na[Ac]) and sodium thiocyanate (Na[SCN]). Sodium acetate, ammonium acetate, chloride and thiocyanate were all provided by Sigma-Aldrich with a purity superior to 99.0 %, 98.0 %, 99.5 % and 99.0 %, respectively. Sodium thiocyanate was provided by Fluka with a purity superior to 98.0 %. Ammonium ethane sulfonate was synthesized, the details are explained in our previous work.[18]

The ionic liquid 1-ethyl-3-methylimidazolium acetate ($[C_2MIM][Ac]$) was purchased from Iolitec with a mass fraction purity of ≥ 98 %. To reduce the water and other volatile substances contents, vacuum (10^{-1} Pa) and moderate temperature (no more than 318.15 K) were always applied to the ionic liquid for at least 2 days prior to their use. After drying, the ionic liquid purity was checked by ^{1}H NMR. Karl Fischer coulometric titration (Metrohm 831 KF Coulometer) was used to determine the final water mass fraction of the ionic liquid, which contained around 6000 ppm of water.

IL + IS samples

The binary mixtures of $[C_2MIM][Ac]$ + IS were prepared in the range of 0 to 0.45 in IS mole fraction, taking into account the solubility limits of each IS, determined on our previous work.[19] The samples were prepared in an inert-atmosphere glove box, since the ionic liquid is moisture sensitive, using an analytical high-precision balance with ± 10^{-5} g accuracy by weighing known masses of the each component into stoppered flasks. Good mixing was assured by magnetic stirring.

NMR spectrometry

All NMR experiments were performed using a Bruker Avance III 400 operating at 400.15 MHz for protons, equipped with a 5 mm high-resolution BBFO probe and with a pulsed field gradient unit, capable of producing magnetic field pulsed gradients in the z-direction of 0.54 T·m^{-1}. The samples were prepared by transferring approximately 2 mL of each IL + IS mixture to 5 mm NMR tubes. For the recording of all spectra, a capillary with deuterated dimethyl sulfoxide (DMSO-d_6) was inserted inside the tube for field-frequency lock and NMR internal reference. The structures and numbering of the IL and ISs are depicted in Figure 1.

The changes in the ^{1}H chemical shifts of $[C_2MIM][Ac]$ with increasing IS concentration, were analyzed. The 1H spectra experiments were carried out at 298.15 K with 8 scans and 4 dummy scans. The ^{1}H NMR spectra of each one of the six IL + IS systems and their respective chemical shifts are depicted in Figures S1-S5 and in Table S1, respectively in the ESI.

NOESY data were acquired for the most concentrated samples of each system. An initial screening of different mixing times was previously performed in order to assure the NOE effect was obtained. For the NOESY data obtained, a mixing time of 300 ms

Fig. 1 Chemical structure and numbering of the ionic liquid and inorganic salts used in this work. a) 1-ethyl-3-methylimidazolium, b) ammonium acetate, c) ammonium chloride, d) ammonium ethane sulfonate, e) ammonium thiocyanate, f) sodium acetate, g) sodium thiocyanate.

was selected and the spectra was obtained with 4 scans and 4 dummy scans at 298.15 K.

For the determination of the ion self-diffusion coefficients of the IL + IS systems, the ^{1}H diffusion coefficients were measured using the pulsed gradient stimulated echo (PGSTE) pulse sequence at 323.15 K (to lower the viscosity into a convenient range). Typically, in each experiment 32 spectra of 32 K data points were collected, with values for the duration of the magnetic field pulsed gradients (δ) of 6.0 ms, diffusion times (Δ) of 500 to 1000 ms, and an eddy current delay set to 5 ms. The gradient recovery time was 200 ms. The sine shaped pulsed gradient (g) was incremented from 5 to 95 % of the maximum gradient strength in a linear ramp. The ion self-diffusion coefficients for the cation and anions in the IL + IS systems were calculated using the integrals of the NMR signal and the Stejskal-Tanner equation. The standard relative deviation obtained for the ion- self-diffusion coefficients was 0.37 % for the neat IL and ranged between 0.58 % and 1.68 % for the mixtures.

Raman spectrometry

Raman spectra of all samples were measured with 1064 nm excitation (Nd-YAG cw laser) using an RFS 100/S (Bruker Optics, Ettlinger, Germany) Fourier-transform Raman spectrometer. Laser power was set to 400 mW and 100 scans were recorded for each sample at room-temperature.

DFT calculations

The geometries of the ion-pairs of the ISs $[NH_4][Ac]$, $[NH_4]Cl$, $[NH_4][SCN]$, $[NH_4][EtSO_3]$, Na[SCN], and Na[Ac] were fully conformationally screened at the M06-2X/aug-cc-pVDZ level of theory. For the ionic liquid $[C_2MIM][Ac]$, the optimized geometry presented by Chen et al.[20] was used. The geometries of the 4 ion cluster structures (IL + IS) were optimized at the same level of theory. The ethanol dielectric constant was used in the optimization of all the structures (ion-pairs and clusters), in order to help mimic the IL media. Furthermore, the electronic energies were improved by calculation of the single point energies at a higher level of theory, the MP2/aug-cc-pVDZ, and also by adding the zero-point vibrational correction value, that was computed at the M06-2X/aug-cc-pVDZ level of theory. The obtained data for the IL, ISs and clusters as well as all the conformations screened, are depicted in Tables S3 and S4 and Figures S9-15.

Table 1 presents the binding energy between the IL and IS molecules, ΔE, that was calculated by the following expression: $\Delta E = E_{cluster} - (E_{IL} + E_{IS})$, where $E_{cluster}$, E_{IL} and E_{IS} are the sum of electronic energy and zero-point values of the cluster, the ionic liquid ion-pair and the inorganic salt ion-pair at their lower energy conformations, respectively.

For this study the GAUSSIAN 09 [21] quantum chemical package was used.

MD calculations

All molecular dynamic simulation where performed with DLPOLY 4.07.[22] The CL&P[23] and OPLS-AA force fields[24] were used to describe the $[C_2MIM][Ac]$ ionic liquid, while a previously recommended parameterization[25] was used to model the $[NH_4]^+$ and $[SCN]^-$ ions. The MD runs were performed at 0.1MPa and 373.15 K, under the isotropic isothermal–isobaric ensemble (*N-p-T*). The temperature and pressure were controlled using Nosé–Hoover thermostats/barostats, with relaxation time constants of 1 and 4 ps, respectively. In all calculations a cutoff distance of 1.4 nm was applied, with the Ewald summation technique (*k*-values set to 16 and α = 0.27107 Å) used to account for interactions beyond this limit. All simulations were prepared with the DLPGEN program,[26] by distributing the molecules in expanded boxes that were subsequently equilibrated to constant density. Besides the simulation of pure $[C_2MIM][Ac]$, two mixtures of this IL with $[NH_4][Ac]$ and $[NH_4][SCN]$ at molar fractions 0.10 and 0.33 were investigated. All simulation boxes were composed by 900 ions (450 ion pairs). The production stages consisted of 10 ns runs, performed with a time step of 2 fs, where the simulation box configurations were recorded each 2 ps.

Results and discussion

Spectroscopic measurements

The changes on the chemical shifts of the IL + IS mixtures can be used in a quantitative way to evaluate the interactions occurring in the bulk system. Therefore, the ^{1}H NMR spectra of each one of the six IL + IS systems were acquired and the chemical shifts' deviations determined as depicted in Figure 2. Although the solubility range of the systems containing sodium-based ISs is smaller, the effect on the IL's chemical shifts in much less pronounced in these systems than in ammonium-based IS, indicating that the interactions between the sodium-based ISs and the IL are weaker than those with ammonium-based ISs.

Moreover, in Figure 2a it can be observed that the protons H2, H4 and H5, belonging to the aromatic ring of the imidazolium, are the most affected by the presence of an IS. These three protons show strong negative deviations, since they undergo an upfield shift, with

Table 1 Binding energies for the IL + IS systems

System	ΔE / kJ·mol^{-1}
$[C_2MIM][Ac]$ + $[NH_4][Ac]$	-64
$[C_2MIM][Ac]$ + $[NH_4]Cl$	-72
$[C_2MIM][Ac]$ + $[NH_4][SCN]$	-83
$[C_2MIM][Ac]$ + $[NH_4][EtSO_3]$	-80
$[C_2MIM][Ac]$ + Na[Ac]	-42
$[C_2MIM][Ac]$ + Na[SCN]	-49

the highest deviation for the H2 proton, the most acidic. The upfield shifts experienced by these aromatic protons indicate that their interactions become weaker as the IS concentration increases. Regarding the other two protons of the imidazolium cation, H6 and H7, they also present negative deviations, although the effect of the IS concentration is much less pronounced. On the other hand, protons H8 (from the terminal -CH_3 of the ethyl chain of the imidazolium cation) and H10 (from the acetate anion) present small positive deviations, i.e. downfield shifts, meaning that they establish stronger interactions upon the addition of the IS to the IL medium.

In general, all studied IL + ammonium-based IS systems show identical behaviour in terms of the up or downfield shifts of the protons. Nevertheless, few differences can be pointed out as the IS's anion is changed: i) for the chloride anion, protons H8 and H10 also display upfield shifts, which is in accordance with the large increase in the viscosity of the system;[18] ii) for the thiocyanate anion, the deviations on the chemical shifts of the protons are higher than those for any other anion, meaning that $[NH_4][SCN]$ is the IS that affects most the IL bulk structure; iii) for the acetate anion, the deviations on the aromatic protons are smaller than for the other ammonium salts, as expected given that there is no new anion present in the mixture.

The same deviation trend observed for the IL protons can now be verified for the ISs in Figure 2b. Regarding the protons of the $[NH_4]^+$ cation, they all present negative deviations, with $[NH_4][SCN]$ presenting the highest and $[NH_4][Ac]$ the lowest. The negative deviations of these protons are somewhat surprising, since we were expecting the ammonium cation to be engaged in interactions, especially with the IL anion. Nevertheless, these results might also mean that the ammonium cation is interacting less with its own counter-ion and thus getting looser in the network. In addition, the deviations of the protons of the ethane sulfonate anion (H12 and H13) are also depicted in Figure 2b, showing very small downfield shifts.

Raman spectroscopy was also employed to probe the molecular environment of the acetate (and thiocyanate) anions by monitoring their frequencies (ν) and bandwidths (Δν). The acetate ion has two vibrational modes, O-C=O and $(H_3)C$-$C(OO^-)$ stretching, at 636cm^{-1} and 900 cm^{-1} respectively, which are in Raman spectra well separated from those of $[C_2MIM]^+$, (Figure S6). The shifts of the $(H_3)C$-$C(OO^-)$ band upon addition of different amounts of IS are shown in Figure 3. It can be seen that the addition of IS to the pure $[C_2MIM][Ac]$ causes frequency upshift and band broadening. The upshifts indicate a stronger bond in the presence of IS, suggesting that the acetate anion becomes less engaged in the interaction with the imidazolium cation. At low concentrations of IS (x_{IS} = 0.10), both bandwidths and frequencies of the acetate band show minor alterations with respect to the neat IL in all IL + IS systems. As the concentration of IS increases (x_{IS} = 0.17), the $\nu_{C\text{-}COO}$ shifts of the systems with $[NH_4][Ac]$, $[NH_4]Cl$ and $[NH_4][EtSO_3]$ are still comparable (when the intensity is normalized, the bands fully overlap), whereas in the system containing $[NH_4][SCN]$, the band undergoes more pronounced broadening and upshift. At the highest concentration of IS (x_{IS} = 0.33), the $\nu_{C\text{-}COO}$ band further upshifts and broadens in all measured mixtures. It can be seen that in the systems containing $[NH_4]Cl$ ($\nu_{C\text{-}COO}$ = 907 cm^{-1}, Δν = 31 cm^{-1}) and $[NH_4][Ac]$ ($\nu_{C\text{-}COO}$ = 904 cm^{-1}, Δν = 26 cm^{-1}) the bandwidths are much larger than in the neat IL ($\nu_{C\text{-}COO}$ = 900 cm^{-1}, Δν = 16 cm^{-1}), suggesting a much more heterogeneous molecular environments of acetate anions. In the system containing $[NH_4][SCN]$ ($\nu_{C\text{-}COO}$ = 914 cm^{-1}, Δν = 19 cm^{-1}), although the bandwidth is not as large as in the other cases, the upshift in the frequency indicates that $[NH_4][SCN]$ is the IS that affects the most the acetate anions. It is noteworthy that the $\nu_{O\text{-}C=O}$ band reveals similar sensitivity towards changes in molecular environment (Figure S6, inset). Furthermore, for the system containing $[NH_4][SCN]$, the molecular environment of thiocyanate was also monitored via the S≡CN stretching mode at 2056 cm^{-1} (data not shown). However, no additional bands, band shifts or broadening were observed in the Raman spectra with the increase in the IS concentration, indicating uniform $[SCN]^-$ environment as previously reported for 1-ethyl-3-methylimidazolium ethyl sulfonate ($[C_2MIM][EtSO_3]$) + $[NH_4][SCN]$.[27]

In Figure 4, the mean orientations of the interacting ions are drawn from NOESY data from the evaluation of the relative strength of the cross peaks found between the four ions in the IL + IS cluster. The NOESY spectra could only be obtained for the ammonium-based ISs because the sodium-based ISs do not present protons in their ions (with the exception of acetate). The relative distance between ions was established using the areas of the cross peaks in the 2D NMR spectra. For all the studied systems, the cross peak with the highest area and the highest proximity between protons belonging to two different ions, was the one corresponding to the cross-relaxation between the protons from the terminal methyl group of the imidazolium (H6) and those in the acetate (H10). The area of this peak was set as reference point, and the areas of all the other peaks were divided by the area of the reference in order to obtain a relative scale of the NOE between the ions in the system.

As depicted in Figure 4, NOESY data suggest that in all systems the acetate anion detaches itself from the imidazolium cation, as it can be evaluated by the low intensity of cross peaks between the acetate anion and the aromatic protons of the imidazolium cation. This is further corroborated by the large downfield shifts recorded in the imidazolium cation, presented in Figure 2a. These results are a direct consequence of the addition of IS to the IL, since it is recognized that in the neat $[C_2MIM][Ac]$ the acetate anions establish in-plane interactions with the three imidazolium ring protons.[28] As the structure of ILs and ISs are both dominated by the

Fig. 2 ^1H NMR chemical shifts deviations for the systems $[C_2MIM][Ac]$ + IS determined at 298.15 K. Each symbol represents a different proton and each IS is represented by a different colour: $[NH_4][Ac]$ blue, $[NH_4]Cl$ green, $[NH_4][EtSO_3]$ red, $[NH_4][SCN]$ orange, Na[Ac] pink, Na[SCN] black. Panels a) and b) illustrate the chemical shift deviations in the IL and in the IS, respectively.

Fig. 3 Raman spectra of $[C_2MIM][Ac]$ + IS systems, acetate C-COO^- stretching region. Each system is represented by a different colour: neat $[C_2MIM][Ac]$ grey; $[NH_4][Ac]$ blue, $[NH_4]Cl$ green, $[NH_4][EtSO_3]$ red, $[NH_4][SCN]$ orange and Na[Ac] pink. The spectra were measured with 1064 nm excitation at 298.15 K.

Coulombic forces, it is expected that the introduction of ISs into the IL media will alter the whole set of interactions that are present, either by the disruption of interactions of the ion-pairs (IL-IL and IS-IS) and/or the establishment of new interactions (IL-IS).

Considering the ammonium cation of the ISs, it can be seen that in all systems there are stronger contacts between this cation and the acetate anion than with any other ion in the mixture. In the case of the $[NH_4][Ac]$ IS, these results were expected since it is not possible to distinguish between the acetate anions from the IL and those belonging to the IS, and hence the high level of contact between the ammonium cation and the acetate anion was anticipated. Regarding the $[NH_4][SCN]$ IS, where the second highest level of contacts was found, the results also support the idea of the establishment of a strong interaction between the $[Ac]^-$ of the IL and the $[NH_4]^+$ of the IS, allowing the other two ions to become more "free". This higher level of interaction of the $[Ac]^-$ anion with the $[NH_4]^+$ cation is consistent with the high downfield shifts of the aromatic protons obtained for this system and depicted in Figure 2a, showing that the imidazolium is interacting less with its own counter-ion (the acetate anion is less engaged, as seen in Figure 3) as the ammonium content in the mixture increases. For the other two ISs ($[NH_4]Cl$ and $[NH_4][EtSO_3]$), similar behaviour to that observed for the $[NH_4][SCN]$ is found, with the low cross peak intensity between the IL's anion and the IS's cation being also consistent with their lower negative deviations in the aromatic protons shown in Figure 2a and the upshifted $\nu_{C\text{-}COO}$ frequencies (Figure 3). In addition, for $[NH_4][EtSO_3]$ it was also possible to obtain the proximity levels to the IS anion. In this case, $[EtSO_3]^-$ anion becomes closer to the IL's ions than to its own counter-ion (the ammonium). Nevertheless these proximity levels are very low, which probably explain the small, yet positive, chemical shift deviations.

The trends obtained from the deviations of the chemical shifts along with the relative contacts determined from the NOESYs are in agreement with the binding energies between the IL and IS molecules obtained from the DFT calculations presented in Table 1. It can be observed that the formation of the four ion cluster is favoured in the case of the ammonium-based ISs, which is consistent with the large deviations depicted in their chemical shifts. For the sodium-based ISs, the ions of the IS prefer to remain associated instead of interacting with those of the IL.

Considering the values of the binding energy (ΔE) for the four ion cluster, it can be observed that for the system containing the

Fig. 4 Preferential interactions between the IL and IS ions for the systems $[C_2MIM][Ac]$ + ammonium-based ISs as derived from NOESY spectra. a) $[NH_4][EtSO_3]$, b) $[NH_4][Ac]$, c) $[NH_4]Cl$ and d) $[NH_4][SCN]$ determined at 298.15 K. The different colours represent the level of relative NOE: very low (0–0.20), low (0.21–0.40), medium (0.41–0.60), high (0.61–0.80) and very high (0.81–1).

$[NH_4][SCN]$ the formation of the cluster is preferred, which is in agreement with the higher deviations of the chemical shifts obtained. In addition, excluding the common ion system, Figure 4 shows that the intensity of the relative NOE between $[NH_4]^+$ and the $[Ac]^-$ in the $[NH_4][SCN]$ containing system, is higher than for the systems with $[NH_4]Cl$ and $[NH_4][EtSO_3]$, which present similar values in terms of their ΔE, chemical shift deviations and levels of proximity between the ions in the system. Regarding the system containing $[NH_4][Ac]$, due to the effect of the common ion, the chemical environment does not change as much as in the case of the other ammonium-based ISs, hence the ΔE and chemical shift deviations are lower.

In Figure 5, the ^1H NMR self-diffusion coefficients (D) for the individual ions of the IL + IS systems are depicted. These results are also presented in Table S2 in the ESI. Unfortunately, due to the lack of protons in some ions of the ISs (Cl^-, $[SCN]^-$ and Na^+), it was not possible to determine the ion self-diffusion coefficients of all species. Moreover, for some concentrations, the $[NH_4]^+$ cation peak overlapped with the H4 and H5 peaks of the imidazolium ring, making impossible the determination of $D[NH_4]^+$.

Nevertheless, some general trends can be established. First, it can be seen that $[NH_4]^+$ has slightly higher diffusivity than $D[C_2MIM]^+$, except for the most concentrated mixtures. With the increase in the amount of IS in the mixture, the $D[NH_4]^+$ starts to decrease to the point it becomes lower than $D[C_2MIM]^+$. This behaviour can be correlated with the approximation between $[NH_4]^+$ and $[Ac]^-$ and the establishment of aggregates between the two (vide infra). Since $[NH_4]^+$ is a smaller and thus more mobile than $[C_2MIM]^+$ or $[Ac]^-$, higher D would be expected. However, with the increase in amount of IS, the formation of aggregates involving $[NH_4]^+$ increases, making the $[NH_4]^+$ less mobile than $[C_2MIM]^+$.

Regarding the IL's diffusion coefficients, Figure 5 shows that the D of the cation (D_{IL}^+) is always higher than of the anion (D_{IL}^-), either in the neat IL or in the mixtures. Previous studies on the diffusion of $[C_2MIM][Ac]$ [28, 29] also showed that the smaller acetate anion diffuses more slowly than the larger imidazolium cation. The results obtained in this work are comparable to those in literature, showing relative standard deviations of 1.6 % and 0.7 % for the D_{IL}^+ and of 0.8 % and 4.4 % for the D_{IL}^- regarding the data presented by Remsing et al.[29] and Bowron et al.[28], respectively.

Fig. 5 ^{1}H NMR self-diffusion coefficients of the ions $[C_2MIM]^+$ (●), $[Ac]^-$ (■), $[NH_4]^+$ (▲) and $[EtSO_3]^-$ (×) in the $[C_2MIM][Ac]$ + IS systems determined at 323.15 K. Each colour represent a different system: IL + $[NH_4][Ac]$ is blue, IL + $[NH_4]Cl$ is green, IL + $[NH_4][EtSO_3]$ is red, IL + $[NH_4][SCN]$ is orange, IL + Na[Ac] is pink and IL + Na[SCN] is black.

Other general trend that can be withdrawn from the diffusion measurements is that, with the exception of the system containing $[NH_4][SCN]$, both the D_{IL}^+ and D_{IL}^- decrease with the IS concentration. Literature shows that this behaviour is common to other IL + IS systems, namely those involving bis(trifluoromethylsulfonyl)amide-based (NTf_2) or bis(fluorosulfonyl)amide-based (FSA) ILs + $[Li][NTf_2]$ or [Li][FSA] respectively,[12, 30-33] systems of *N*,*N*-diethyl-*N*-methyl-*N*-(2-methoxyethyl)ammonium (DEME) based ILs with lithium ISs, $[DEME][BF_4]$ + $[Li][BF_4]$ and $[DEME][CF_3BF_3]$ or $[NTf_2]$ + $[Li][NTf_2]$,[34] and also the system of $[C_2MIM][BF_4]$ + $[Li][BF_4]$ [35] where the addition of IS leads to the decrease of both D_{IL}^+ and D_{IL}^-.

In this study, the decrease observed in both D_{IL}^+ and D_{IL}^- follows the trend Na[Ac] > $[NH_4]Cl$ > Na[SCN] > $[NH_4][EtSO_3]$ > $[NH_4][Ac]$ > $[NH_4][SCN]$, where the next to the last one is the IS where a smallest decrease in the D_{IL} was obtained; for $[NH_4][SCN]$, D_{IL}^- decreases and D_{IL}^+ increases upon the addition of IS. This decrease in ion mobility with the IS concentration is in agreement with our previous studies,[18] where an increase in the concentration of the IS led to the decrease of the ionic conductivity (with the exception of $[NH_4][SCN]$ where the conductivity increased with the addition of IS). Interestingly, neither of these trends (diffusion and ionic conductivity) follow the behaviour of the viscosity.[18] The systems containing the ISs $[NH_4][EtSO_3]$ and $[NH_4]Cl$ present the highest increase in viscosity, which should result in lower *D* for these systems, according to the Stokes-Einstein (SE) equation (equation 1) where it is assumed that the diffusing species are rigid spheres in a continuum of a solvent.[36]

$$D = \frac{k_B T}{c\pi\eta r} \quad (1)$$

where k_B is the Boltzmann constant, *T* is the temperature, η is the viscosity, *r* is the Stokes radius and *c* is a constant dependent on the strength of the interactions between the diffusing species and the medium, that usually ranges between 4 and 6 for slip and stick boundary conditions, respectively. Nevertheless, several studies on ILs have shown that the *c* value for these fluids could be lower than 4.[33, 34, 37]

In order to further explore this divergence, the diffusion data obtained in this work was correlated with the viscosity data of our previous study.[18] Figure S7 in the ESI, plots the *D* for each ion in the system versus the $k_BT/\pi\eta_{mix}$, where linear relationships ($r^2 \geq 0.99$) were only obtained for the $[Ac]^-$ anion (in all system) and for the $[C_2MIM]^+$ cation in the system containing Na[Ac]. However, in the $[C_2MIM][Ac]$ + ammonium-based ISs systems, no linearity was obtained. It is particularly the case of $[NH_4][SCN]$, in which the D_{IL}^+ increases with the increase in viscosity and the D_{IS}^+ does not decrease in a linear way. These findings are different from the results reported by Hayamizu et al.[31], who obtained linear plots for all ions in the studied IL + IS mixture, thus allowing the use of the SE equation to obtain physical insights between the diffusional motion of the species and the viscosity. In the present work, the application of the SE equation is not valid. In fact, the validity of the SE equation for neat ILs is being debated by other authors .[38, 39]

Concerning the ion self-diffusion coefficients of the IS, we observed that the increase in the IS concentration also leads to the decrease of both D_{IS}^+ and D_{IS}^-, again with the exception of $[NH_4][SCN]$. This trend is better illustrated in Figure S8 in the ESI, where the ratio between the self-diffusion coefficients of each ion and the D_{IL}^+ is plotted against the molar fraction of IS.

For the system with the IS $[NH_4][EtSO_3]$, it was possible to determine the D_{IS}^-. It can be seen that at lower IS concentrations the $D_{[EtSO3]}^-$ is smaller than $D_{[Ac]}^-$ and as the concentration of IS increases $D_{[EtSO3]}^-$ becomes higher than $D_{[Ac]}^-$. Moreover, it can also be seen that the addition of IS always affects more the D_{IL}^- than the D_{IL}^+ (D_{IL}^- / D_{IL}^+ always < 1).

Molecular Dynamics simulations

To gain further insight into the structure of $[C_2MIM][Ac]$ + IS mixtures, several molecular dynamic simulations were performed, for the ISs $[NH_4][Ac]$ and $[NH_4][SCN]$. The selection of these two ISs is related with the irregular behaviour observed in the physical properties of IL + $[NH_4][SCN]$ mixtures relative to the other salts, presented above, while $[NH_4][Ac]$ was chosen to represent the most common trends observed when ISs are added to the IL. Figure 6 shows the probability, $P(n_a)$, of finding an aggregate of size n_a, computed from the MD simulation results with the methodology previously described.[40, 41] In Figure 6a it is observed that the size variation of the aggregates formed by $[NH_4]^+$ and $[Ac]^-$ does not change monotonically. Instead, several probability maxima are found for aggregates with a particular size. This occurs because the ammonium cations tend to be surrounded by ~ 4 $[Ac]^-$ anions (Figure 6d), while acetate, on average, are in contact with less than one $[NH_4]^+$ cation (considering the data for x_{IS} = 0.1). This suggests the formation of isolated clusters composed by ~ 5 ions, as illustrated in Figure 7. Thus, any time an anion produces a bridge between two $[NH_4]^+$ cations, the size of the aggregate changes in accordance to the number of acetate ions connected to the two cations, given rise to a high probability of finding aggregates with a specific size. This observation is in good agreement with the spectroscopic findings reported above, that preferential interaction exists between the ammonium and acetate ions. This interaction is sustained by the formation of hydrogen bonds (H-bonds), that

Fig. 7 Snapshot of an aggregate of $[NH_4]^+$ cation surrounded by acetate ions, found in a mixture of $[C_2MIM][Ac]$ with $[NH_4][SCN]$ at x_{IS} = 0.10 and T = 373.15 K.

according to Jeffrey's hydrogen bond distance criteria,[42] are relatively strong (strong and moderate H-bonds exist when H···O distances vary in the range 2.2 − 2.5 Å and 2.5 − 3.2 Å, respectively; see distances in Figure 7).

The analysis of Figures 6b and 6c shows a strong interaction between $[C_2MIM]^+$ and $[SCN]^-$ (these two ions are able to produce long polar networks, with the thiocyanate and imidazolium ions surrounded by ~ 4 and ~ 2 counterions, respectively; Figure 6d) and an almost absence of contact between the IS ions (with an average number of neighbours for each ion bellow 0.6, Figure 6d). This suggest a strong interaction between the IS ions and the IL polar network. Figure 6a also reveals that the aggregates formed between $[NH_4]^+$ and $[Ac]^-$ ions when $[NH_4][SCN]$ is added to the ionic liquid tend to be larger than in the case of $[NH_4][Ac]$. This observation suggests a stronger interaction between the former IS and the IL bulk structure, in accordance to the higher chemical shifts discussed above, observed when $[NH_4][SCN]$ is mixed with $[C_2MIM][Ac]$.

Ionicity

The ionicity of ILs has been interpreted as a ratio between the effective concentration of charged species and the total concentration of the IL, measuring the dissociativity or degree of correlative motion of ions.[43, 44] There are two main methods to estimate the ionicity of ILs. The first is based on the Walden Plot approach, where plots made of the logarithm of the molar conductivity against the logarithm of the fluidity are drawn. In these plots, the ideal Walden line is given by a straight line with a unitary slope, drawn with data of an aqueous solution of KCl, which is usually considered to be representative of the ideal electrolyte, where the ions are known to be fully dissociated. The quantitative determination of the ionicity of the IL is given by the distance of the IL's data to the ideal Walden line. However, this method has been criticized due to the use of KCl solutions of arbitrary compositions as a reference, since Schreiner et al.[45] observed that the slopes of Walden plots for KCl solutions do not represent the unity. In addition, the use of the Walden plot as a quantitative method for the ionicity has also been questioned in the case of a weak electrolyte, where the degree of dissociation is determined by the pK_a, which is a thermodynamic quantity.[46] Nevertheless, from a qualitative point the deviation from the ideal Walden line (ΔW) is still a versatile tool to access the ionicity of ILs.

In our recent study,[18] we used the ΔW to determine of the ionicity of the same IL + IS systems studied in this work and compared them to the ionicity calculated by other method proposed by Ueno et al.[47], also based on the Walden plot approach. In this last method the ionicity is defined as the ratio between the molar conductivity, calculated from the ionic conductivity measured by the electrochemical impedance method (Λ_{imp}), and the ideal molar conductivity (Λ_{ideal}), which is assumed to be equal to the fluidity (in $Poise^{-1}$) taken from the ideal Walden line. The results proved to be consistent from a qualitative point of view: the addition of ammonium-based ISs increased the ionicity of the $[C_2MIM][Ac]$ IL, while the sodium-based ISs decreased it.

The second and most consensual method used for the quantitative determination of the ionicity uses the ratio between the Λ_{imp}, that accounts for the migration of charged species in an electric field, and the molar conductivity calculated from the ion self-diffusion coefficients (Λ_{NMR}), that accounts for the migration of all species in the media (charged and neutral, ions and aggregates).[44] The value of Λ_{NMR} is determined by the Nernst-Einstein (NE) equation as follows:

$$\Lambda_{NMR} = \frac{F^2}{R \cdot T}\left(D^+ + D^-\right) \quad (2)$$

where R and F are the gas and Faraday constants, respectively, T is the temperature and $D^{+/-}$ are the ion self-diffusion coefficients of the IL obtained from the NMR. However, in a IL + IS binary systems, the mole fractions (x) of the IL and the IS have to be accounted for, as follows:

$$\Lambda_{NMR} = \frac{F^2}{R \cdot T}\left(x_{IL}D_{IL}^+ + x_{IL}D_{IL}^- + x_{IS}D_{IS}^+ + x_{IS}D_{IS}^-\right) \quad (3)$$

Since in the determination of the diffusion by NMR, D accounts for all species in solution, both free and associated forms, the value of Λ_{NMR} is always overestimated.[31] Thus, the ratio Λ_{imp} / Λ_{NMR} will always be smaller than the unity.[44] In this study, the determination of the D of all ions was only possible in the systems with the ISs $[NH_4][Ac]$ and $[NH_4][EtSO_3]$, the calculation of the ionicity through the Λ_{imp} / Λ_{NMR} ratio was only accomplished for two IL + IS systems.

Figure 8 represents a comparison between the ionicity calculated using two different methods, the Λ_{imp} / Λ_{ideal} ratio and the Λ_{imp} / Λ_{NMR} ratio. The obtained results demonstrate opposite trends, showing that the addition of the IS to the IL makes the determination of these system's ionicity a challenge. It can be seen

Fig. 6 Probability, $P(n_a)$, of finding an aggregate of size n_a, for mixtures with different molar fraction of $[NH_4][Ac]$ and $[NH_4][SCN]$ with $[C_2MIM][Ac]$, at 373.15 K. Each graphic represents the aggregates formed between a) $[NH_4]^+$ and $[Ac]^-$, b) $[C_2MIM]^+$ and $[SCN]^-$ and c) $[NH_4]^+$ and $[SCN]^-$. d) Average number of counter-ions, N_i, of (×) $[C_2MIM]^+$, (△) $[Ac]^-$, (○) $[SCN]^-$ and (□) $[NH_4]^+$ in different IL + ISs concentrations. The colour of each series denotes the interactions between $[C_2MIM]^+$ and $[Ac]^-$ (red), $[C_2MIM]^+$ and $[SCN]^-$ (green), $[NH_4]^+$ and $[Ac]^-$ (blue) and $[NH_4]^+$ and $[SCN]^-$ (orange). The solid and dashed lines correspond to mixtures with $[NH_4][Ac]$ and $[NH_4][SCN]$, respectively. In order to visualize all data points, a small offset along the x axis was applied. Thus all data correspond to IS molar fractions of 0, 0.10 or 0.33.

that the ionicities calculated trough the Λ_{imp} / Λ_{ideal} ratio increasing upon the addition of IS to the IL, while the ionicities calculated trough the Λ_{imp} / Λ_{NMR} ratio decrease and always presents values lower than the neat IL. However, as discussed above the SE equation is not valid in these systems and therefore trends in Λ_{imp} / Λ_{ideal} may be distorted for this reason. Nevertheless, for the neat IL, $[C_2MIM][Ac]$, the rough consistency between the two methods is confirmed.

The comparison between these two methods had already been made for neat aprotic ILs,[5, 47] protic ILs[48] and glyme-Li salt equimolar mixtures[47] and a rough consistency was observed. In addition, other studies on the ionicity of neat ILs[34, 37, 44] and aqueous solutions of ILs,[49] where Walden plots are drawn and the ionicity calculated from the Λ_{imp} / Λ_{NMR} ratio, have also corroborated the consistency of the results obtained from both methods. However, in another study concerning IL + IS systems, Hayamizu et al.[31] doped ILs *N*-methyl-*N*-propyl-pyrrolidinium (P_{13}) $[NTf_2]$ and [FSA] with a fixed concentration of $[Li][NTf_2]$ and [FSA], respectively, and obtained different trends for the ionicity when the two methods described above are used. Using the Walden plot, the authors verified that the trend in the ΔW was $[P_{13}][NTf_2]$ > $[P_{13}][NTf_2]$ + $[Li][NTf_2]$ > $[P_{13}][FSA]$ + [Li][FSA] > $[P_{13}][FSA]$, with the latter neat IL displaying the highest ionicity, whereas when the ionicity was calculated by the Λ_{imp} / Λ_{NMR} ratio, both IL + IS mixtures yielded higher ionicities than the neat ILs according to the following trend: $[P_{13}][FSA]$ + [Li][FSA] > $[P_{13}][NTf_2]$ + $[Li][NTf_2]$ > $[P_{13}][FSA]$ > $[P_{13}][NTf_2]$. In this study the authors do not explore any further these results. However, these different trends clearly indicate that the determination of the ionicity in IL-IS mixtures is not as simple as in neat ILs and additional studies are needed. This could also be due to the fact that we don't have only a single equilibrium between free ions and aggregate since, with the introduction of the IS, more than one equilibrium are possible between ions.

In addition, Holloczki et al.[50] recently showed that the charge transfer between the ions in neat ILs can also affect the determination of the ionicity, since the neutralization of the mobile species in the media occurs not only due to the formation of ion pairs but also as a result of the charge transfer. Indeed, their data suggested that both phenomena are significant factors that could explain the lower than expected conductivities (Λ_{NMR}). Moreover, these authors also performed MD simulations on a mixture of NaCl in the IL $[C_4MIM]Br$, and showed that by increasing the charge on the ions both the IS and the IL interactions become stronger and the association of the ion pair is favoured, while a decrease of the charge leads to the IL to behave more like a molecular liquid than a salt, showing higher fluidity.

Conclusions

In this work we present insights into the interactions between mixtures of the IL $[C_2MIM][Ac]$ with several ammonium and sodium-based ISs. Our studies reveal that the ammonium based ISs can establish more interactions with the IL than the sodium-based, which was verified by the higher deviations of the ^1H NMR chemical shifts and corroborated by the DFT calculations. We found that these interactions were in part a result of the approximation of the IS's cation, the ammonium, to the IL's anion, the acetate, that lead to the establishment of aggregates and to a more detached imidazolium cation. These effects were more pronounced in the case were the IS was the $[NH_4][SCN]$.

The ion self-diffusion coefficients show that the introduction of IS had a deep effect on the diffusion of the IL's ions, specifically in the case of the imidazolium cation. Moreover, for the systems with $[NH_4][Ac]$ and $[NH_4][EtSO_3]$ ISs, the ionicity was calculated through the Λ_{imp} / Λ_{NMR} ratio and compared with the ionicity determined through the Walden plot approach. The two methods show divergent behaviours meaning that the interplay between the interactions of IL and IS is much more complex than in the case of neat ILs or molten salts.

Acknowledgements

Filipe S. Oliveira gratefully acknowledges the financial support of Fundação para a Ciência e Tecnologia (FCT) through the Ph.D. fellowship SFRH/BD/73761/2010 and Isabel M. Marrucho for a contract under FCT Investigator 2012 Program. The authors also acknowledge FCT for the financial support through the research units GREEN-it "Bioresources for Sustainability" (UID/Multi/04551/2013) and UCIBIO (UID/Multi/04378/2013). The NMR spectrometers are part of The National NMR Facility, supported by FCT (RECI/BBB-BQB/0230/2012). Douglas R. MacFarlane is grateful to the Australian Research Council for funding of his Australian Laureate Fellowship

References

1 D. R. MacFarlane and K. R. Seddon, *Aust. J. Chem.*, 2007, **60**, 3-5.
2 N. V. Plechkova and K. R. Seddon, *Chem. Soc. Rev.*, 2008, **37**, 123-150.
3 L. P. N. Rebelo, J. N. C. Lopes, J. M. S. S. Esperança, H. J. R. Guedes, J. Łachwa, V. Najdanovic-Visak and Z. P. Visak, *Acc. Chem. Res.*, 2007, **40**, 1114-1121.
4 D. R. MacFarlane, M. Forsyth, E. I. Izgorodina, A. P. Abbott, G. Annat and K. Fraser, *Phys. Chem. Chem. Phys.*, 2009, **11**, 4962-4967.
5 H. Tokuda, S. Tsuzuki, M. Susan, K. Hayamizu and M. Watanabe, *J. Phys. Chem. B*, 2006, **110**, 19593-19600.
6 K. Ueno, H. Tokuda and M. Watanabe, *Phys. Chem. Chem. Phys.*, 2010, **12**, 1649-1658.
7 M. Yoshizawa, W. Xu and C. A. Angell, *J. Am. Chem. Soc.*, 2003, **125**, 15411-15419.
8 M. Brüssel, M. Brehm, A. S. Pensado, F. Malberg, M. Ramzan, A. Stark and B. Kirchner, *Phys. Chem. Chem. Phys.*, 2012, **14**, 13204-13215.
9 M. Brüssel, M. Brehm, T. Voigt and B. Kirchner, *Phys. Chem. Chem. Phys.*, 2011, **13**, 13617-13620.

10 Y. Umebayashi, T. Mitsugi, S. Fukuda, T. Fujimori, K. Fujii, R. Kanzaki, M. Takeuchi and S.-I. Ishiguro, *J. Phys. Chem. B*, 2007, **111**, 13028-13032.
11 Y. Umebayashi, S. Mori, K. Fujii, S. Tsuzuki, S. Seki, K. Hayamizu and S.-i. Ishiguro, *J. Phys. Chem. B*, 2010, **114**, 6513-6521.
12 S. Tsuzuki, K. Hayamizu and S. Seki, *J. Phys. Chem. B*, 2010, **114**, 16329-16336.
13 M. C. Corvo, J. Sardinha, S. C. Menezes, S. Einloft, M. Seferin, J. Dupont, T. Casimiro and E. J. Cabrita, *Angew. Chem. Int. Ed.*, 2013, **52**, 13024-13027.
14 Y. Lingscheid, S. Arenz and R. Giernoth, *ChemPhysChem*, 2012, **13**, 261-266.
15 A. Mele, G. Romanò, M. Giannone, E. Ragg, G. Fronza, G. Raos and V. Marcon, *Angew. Chem. Int. Ed.*, 2006, **45**, 1123-1126.
16 A. Mele, C. D. Tran and S. H. De Paoli Lacerda, *Angew. Chem. Int. Ed.*, 2003, **42**, 4364-4366.
17 S. Gabl, O. Steinhauser and H. Weingärtner, *Angew. Chem. Int. Ed.*, 2013, **52**, 9242-9246.
18 F. S. Oliveira, L. P. N. Rebelo and I. M. Marrucho, *J. Chem. Eng. Data*, 2015, **60**, 781-789.
19 A. B. Pereiro, J. M. M. Araújo, F. S. Oliveira, J. M. S. S. Esperança, J. N. C. Lopes, I. M. Marrucho and L. P. N. Rebelo, *J. Chem. Thermodyn.*, 2012, **55**, 29-36.
20 S. Chen, R. Vijayaraghavan, D. R. MacFarlane and E. I. Izgorodina, *J. Phys. Chem. B*, 2013, **117**, 3186-3197.
21 M. J. Frisch, G. W. Trucks, H. B. Schlegel, G. E. Scuseria, M. A. Robb, J. R. Cheeseman, G. Scalmani, V. Barone, B. Mennucci and G. A. Petersson, Wallingford, CT, 2009.
22 I. T. Todorov, W. Smith, K. Trachenko and M. T. Dove, *J. Mater. Chem.*, 2006, **16**, 1911-1918.
23 J. N. C. Lopes, J. Deschamps and A. A. H. Pádua, *J. Phys. Chem. B*, 2004, **108**, 2038-2047.
24 W. L. Jorgensen, D. S. Maxwell and J. TiradoRives, *J. Am. Chem. Soc.*, 1996, **118**, 11225-11236.
25 A. B. Pereiro, J. M. M. Araujo, F. S. Oliveira, C. E. S. Bernardes, J. M. S. S. Esperanca, J. N. Canongia Lopes, I. M. Marrucho and L. P. N. Rebelo, *Chem. Commun.*, 2012, **48**, 3656-3658.
26 C. E. S. Bernardes and A. Joseph, *J. Phys. Chem. A*, 2015, **119**, 3023-3034.
27 F. S. Oliveira, A. B. Pereiro, J. M. M. Araujo, C. E. S. Bernardes, J. N. Canongia Lopes, S. Todorovic, G. Feio, P. L. Almeida, L. P. N. Rebelo and I. M. Marrucho, *Phys. Chem. Chem. Phys.*, 2013, **15**, 18138-18147.
28 D. T. Bowron, C. D'Agostino, L. F. Gladden, C. Hardacre, J. D. Holbrey, M. C. Lagunas, J. McGregor, M. D. Mantle, C. L. Mullan and T. G. A. Youngs, *The Journal of Physical Chemistry B*, 2010, **114**, 7760-7768.
29 R. C. Remsing, G. Hernandez, R. P. Swatloski, W. W. Massefski, R. D. Rogers and G. Moyna, *J. Phys. Chem. B*, 2008, **112**, 11071-11078.
30 O. Borodin, G. D. Smith and W. Henderson, *J. Phys. Chem. B*, 2006, **110**, 16879-16886.
31 K. Hayamizu, S. Tsuzuki, S. Seki, K. Fujii, M. Suenaga and Y. Umebayashi, *J. Chem. Phys.*, 2010, **133**, 1945051-19450513.
32 K. Hayamizu, S. Tsuzuki, S. Seki, Y. Ohno, H. Miyashiro and Y. Kobayashi, *J. Phys. Chem. B*, 2008, **112**, 1189-1197.
33 K. Hayamizu, S. Tsuzuki, S. Seki and Y. Umebayashi, *J. Chem. Phys.*, 2011, **135**, 0845051-08450511.
34 K. Hayamizu, S. Tsuzuki and S. Seki, *J. Chem. Eng. Data*, 2014, **59**, 1944-1954.
35 K. Hayamizu, Y. Aihara, H. Nakagawa, T. Nukuda and W. S. Price, *J. Phys. Chem. B*, 2004, **108**, 19527-19532.
36 E. L. Cussler, *Diffusion mass transfer in fluid systems 2nd ed.*, Cambridge University Press, Cambridge, UK, 1997.
37 B. E. M. Tsamba, S. Sarraute, M. Traikia and P. Husson, *J. Chem. Eng. Data*, 2014, **59**, 1747-1754.
38 T. Koeddermann, R. Ludwig and D. Paschek, *ChemPhysChem*, 2008, **9**, 1851-1858.
39 A. W. Taylor, P. Licence and A. P. Abbott, *Phys. Chem. Chem. Phys.*, 2011, **13**, 10147-10154.
40 C. E. S. Bernardes, M. E. Minas da Piedade and J. N. Canongia Lopes, *J. Phys. Chem. B*, 2011, **115**, 2067-2074.
41 K. Shimizu, C. E. S. Bernardes and J. N. Canongia Lopes, *J. Phys. Chem. B*, 2014, **118**, 567-576.
42 G. A. Jeffrey, *An introduction to hydrogen bonding*, Oxford University Press: New York, 1997.
43 C. Zhang, K. Ueno, A. Yamazaki, K. Yoshida, H. Moon, T. Mandai, Y. Umebayashi, K. Dokko and M. Watanabe, *J. Phys. Chem. B*, 2014, **118**, 5144-5153.
44 K. Ueno, H. Tokuda and M. Watanabe, *Phys. Chem. Chem. Phys.*, 2010, **12**, 1649-1658.
45 C. Schreiner, S. Zugmann, R. Hartl and H. J. Gores, *J. Chem. Eng. Data*, 2010, **55**, 1784-1788.
46 K. R. Harris, *J. Phys. Chem. B*, 2010, **114**, 9572-9577.
47 K. Ueno, K. Yoshida, M. Tsuchiya, N. Tachikawa, K. Dokko and M. Watanabe, *J. Phys. Chem. B*, 2012, **116**, 11323-11331.
48 M. S. Miran, H. Kinoshita, T. Yasuda, M. A. B. H. Susan and M. Watanabe, *Phys. Chem. Chem. Phys.*, 2012, **14**, 5178-5186.
49 J. M. Andanson, M. Traikia and P. Husson, *J. Chem. Thermodyn.*, 2014, **77**, 214-221.
50 O. Holloczki, F. Malberg, T. Welton and B. Kirchner, *Phys. Chem. Chem. Phys.*, 2014, **16**, 16880-16890.

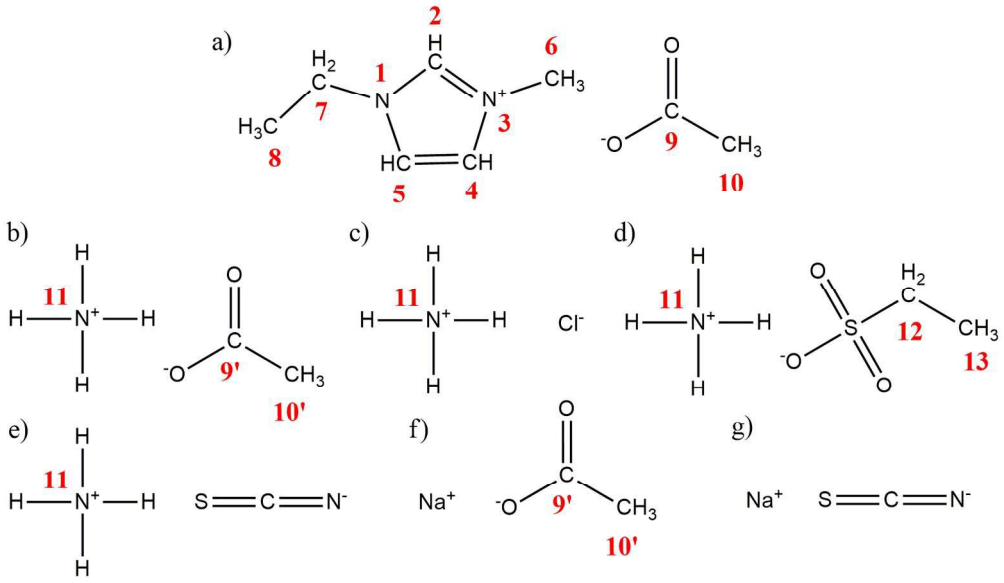

160x93mm (300 x 300 DPI)

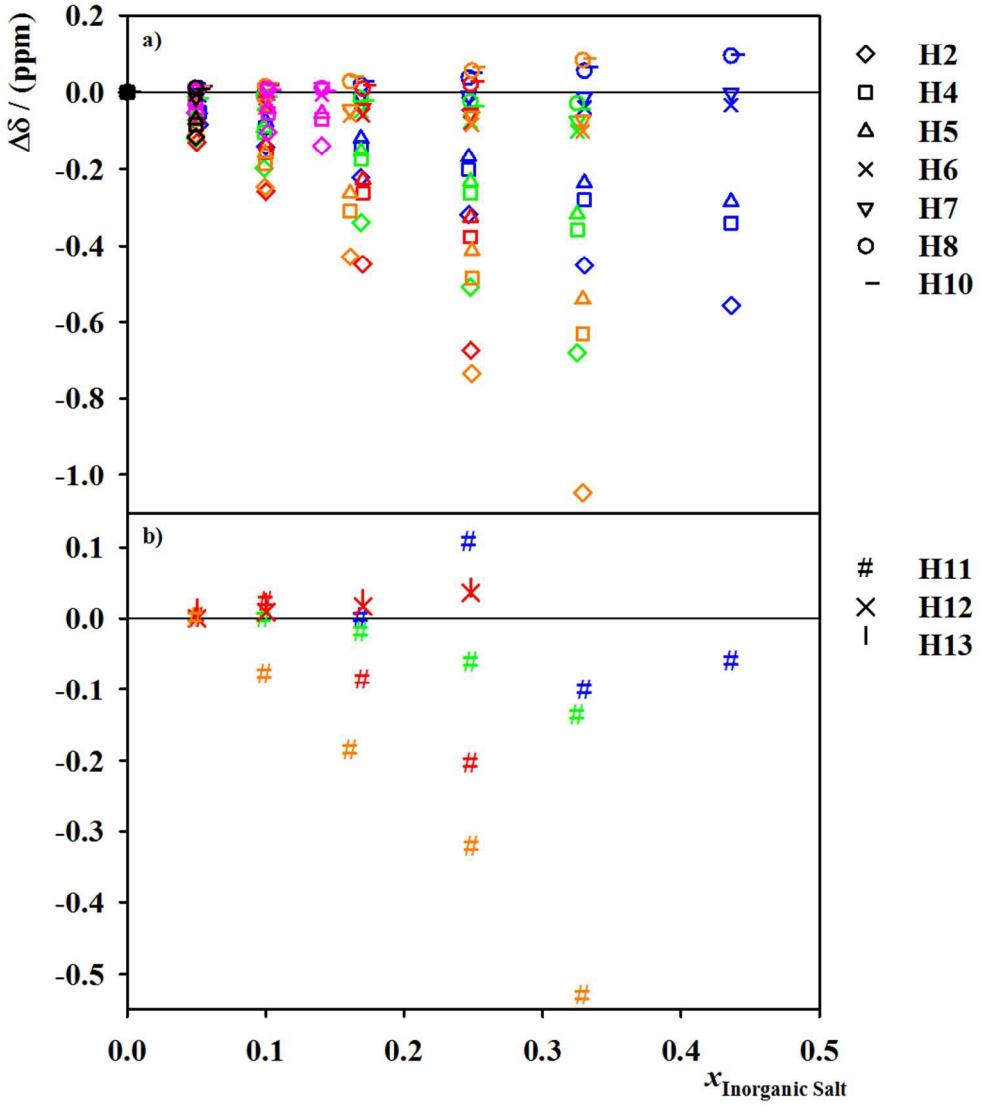

180x210mm (150 x 150 DPI)

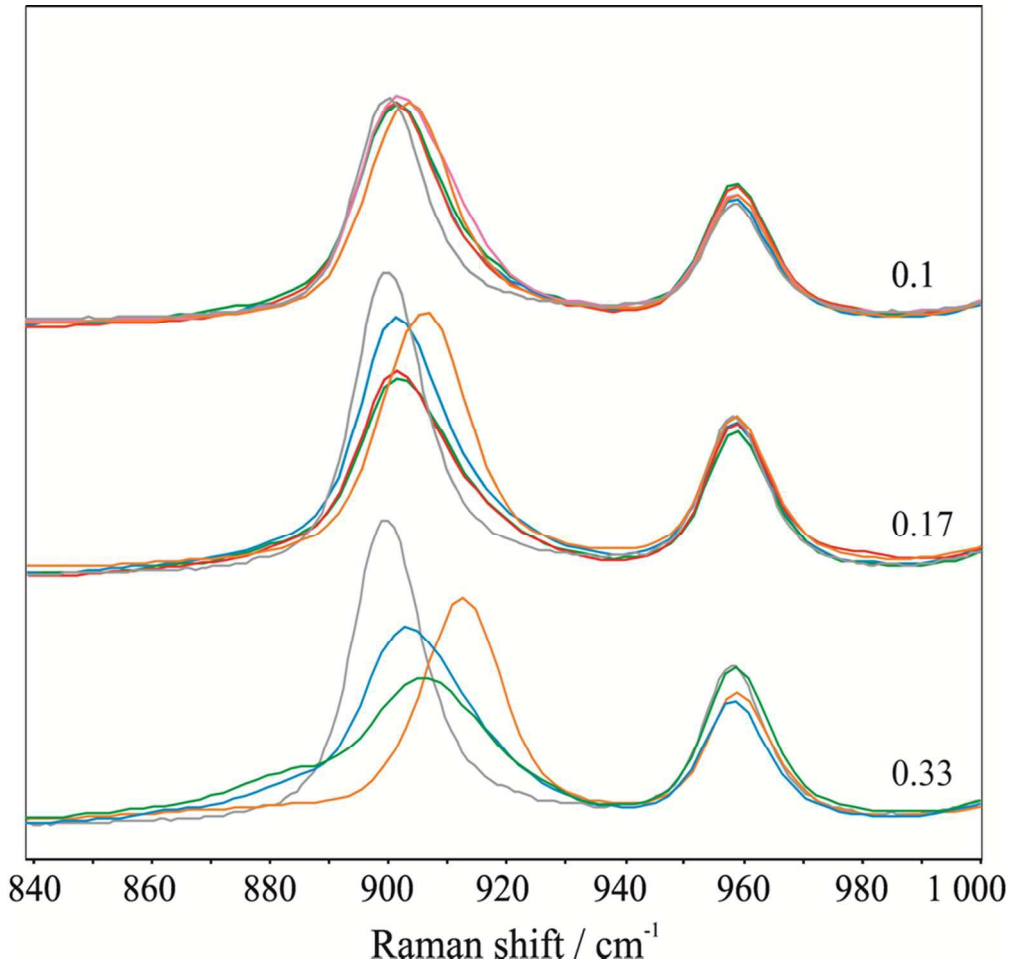

85x80mm (300 x 300 DPI)

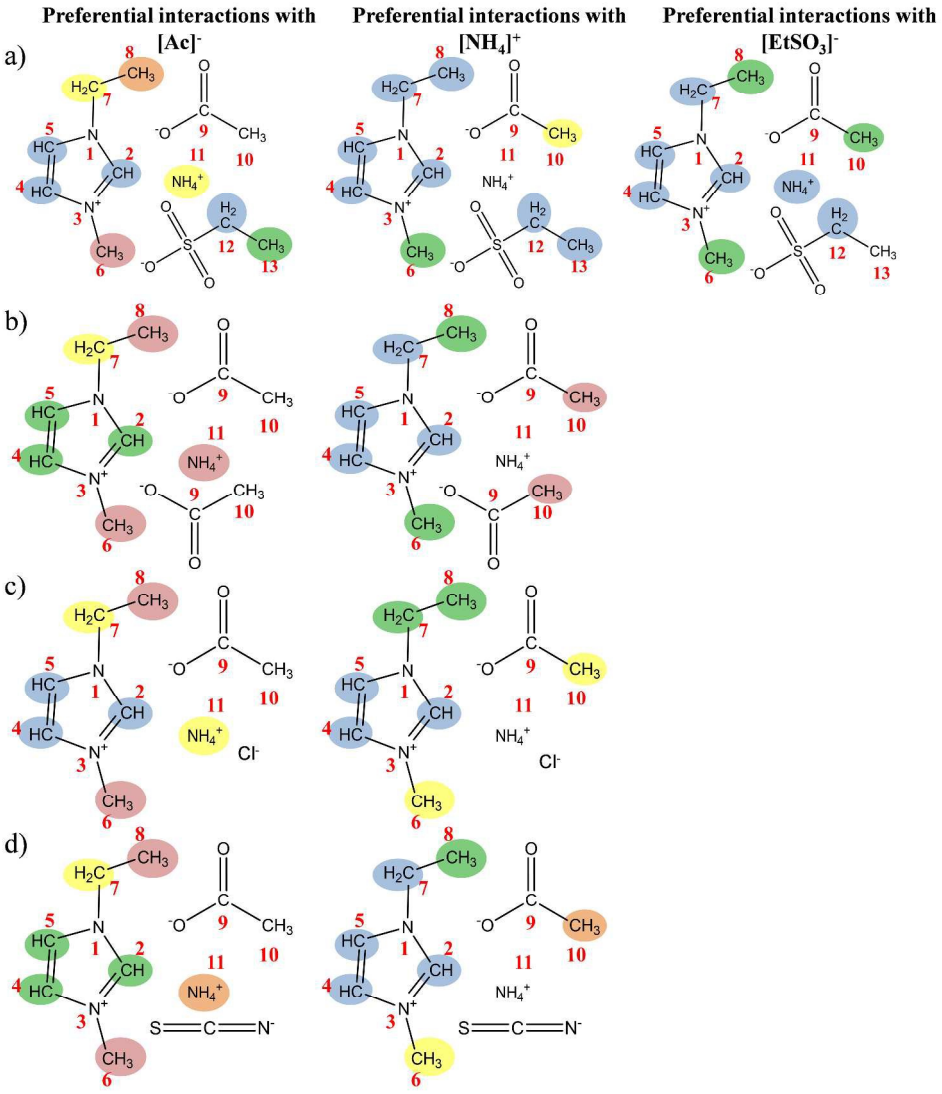

1412x1558mm (96 x 96 DPI)

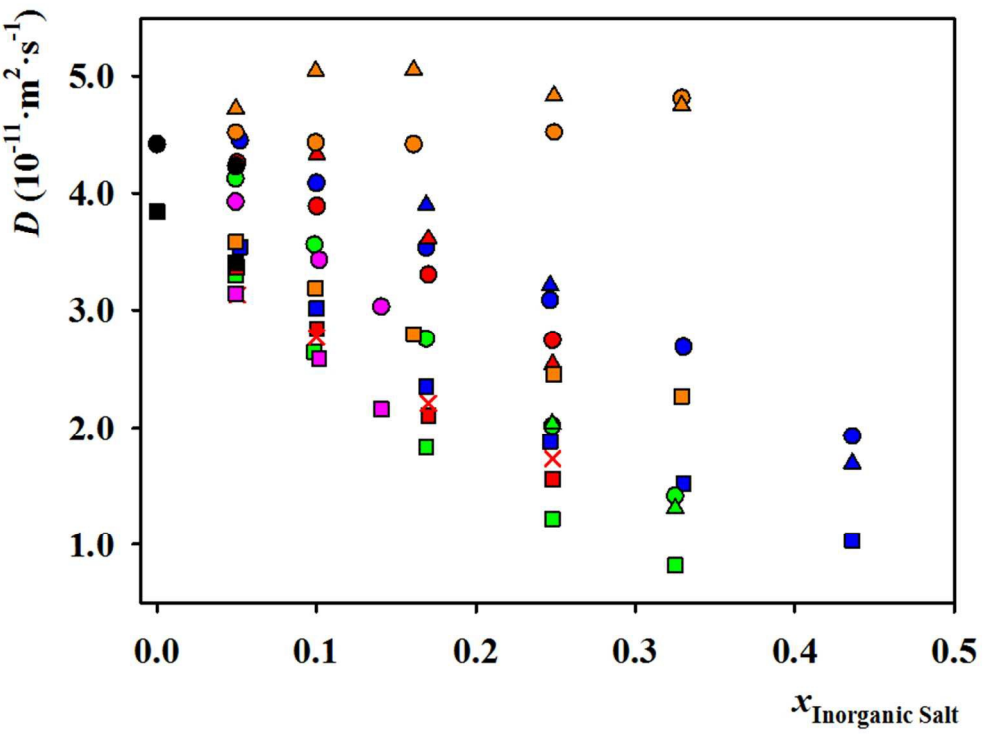

153x123mm (150 x 150 DPI)

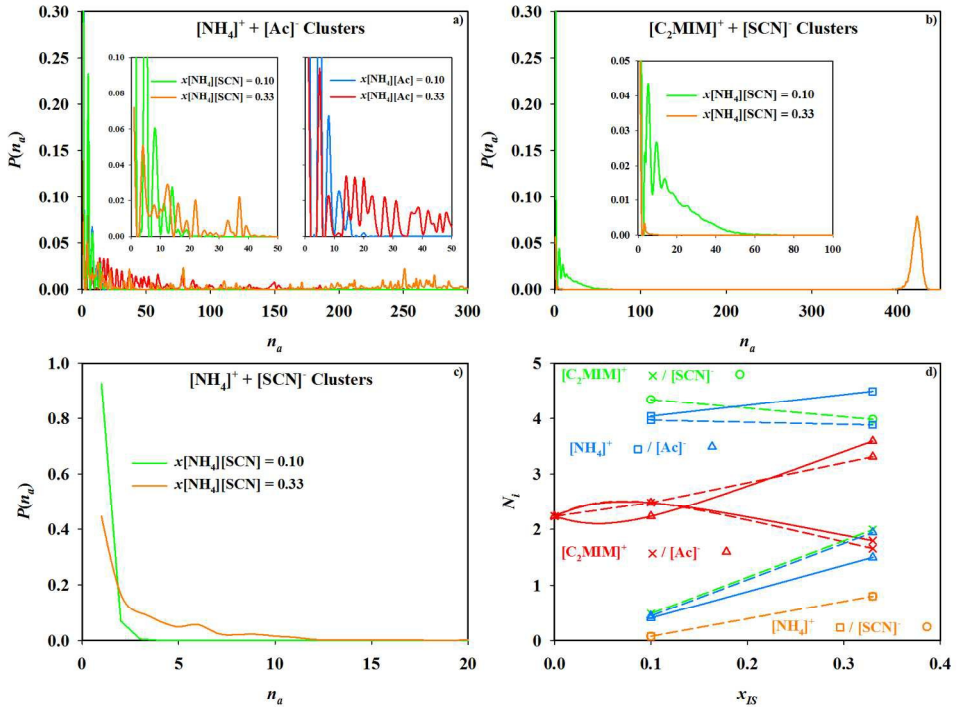

323x233mm (150 x 150 DPI)

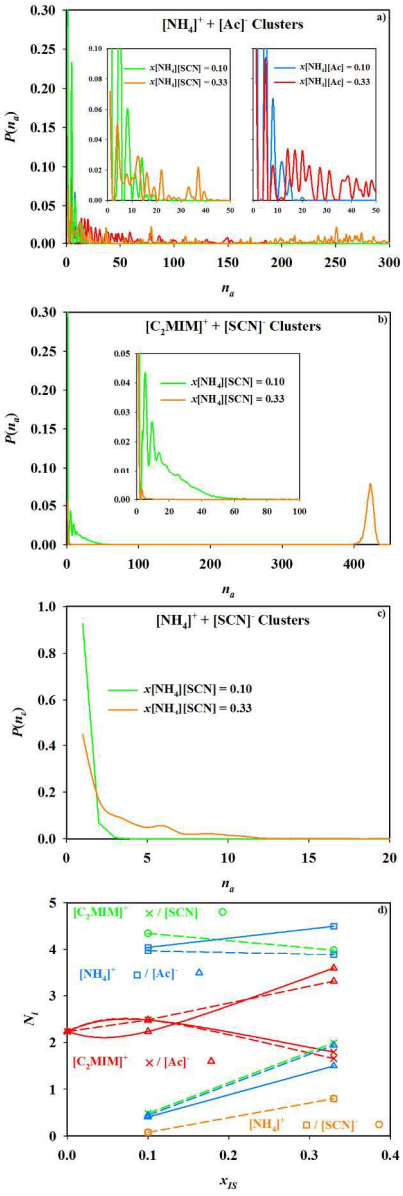

171x462mm (150 x 150 DPI)

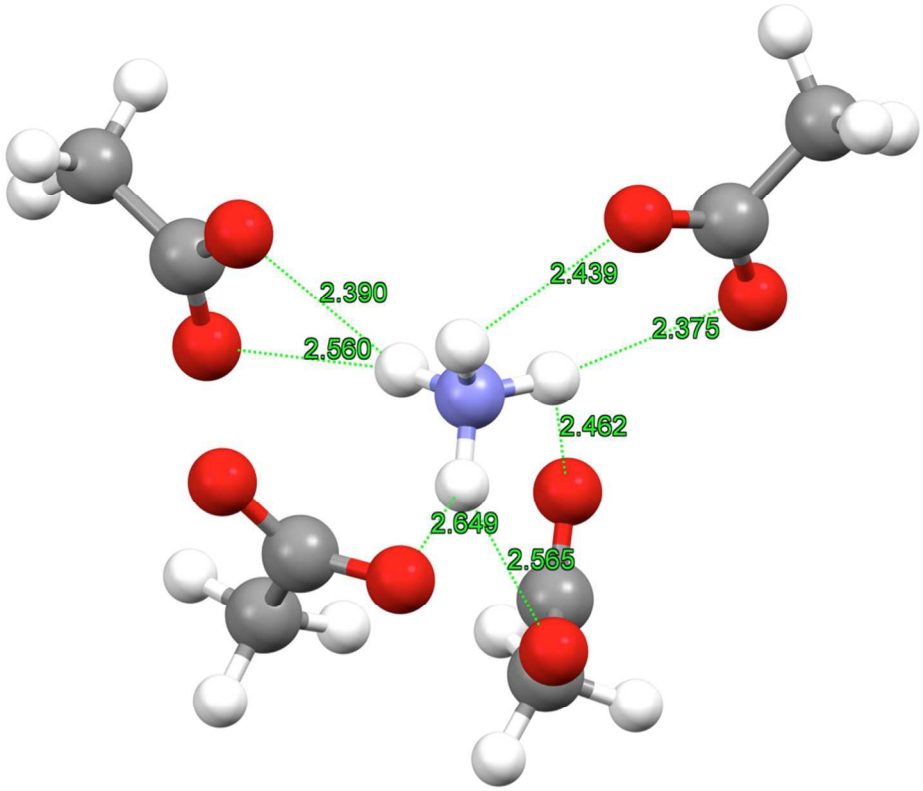

425x348mm (72 x 72 DPI)

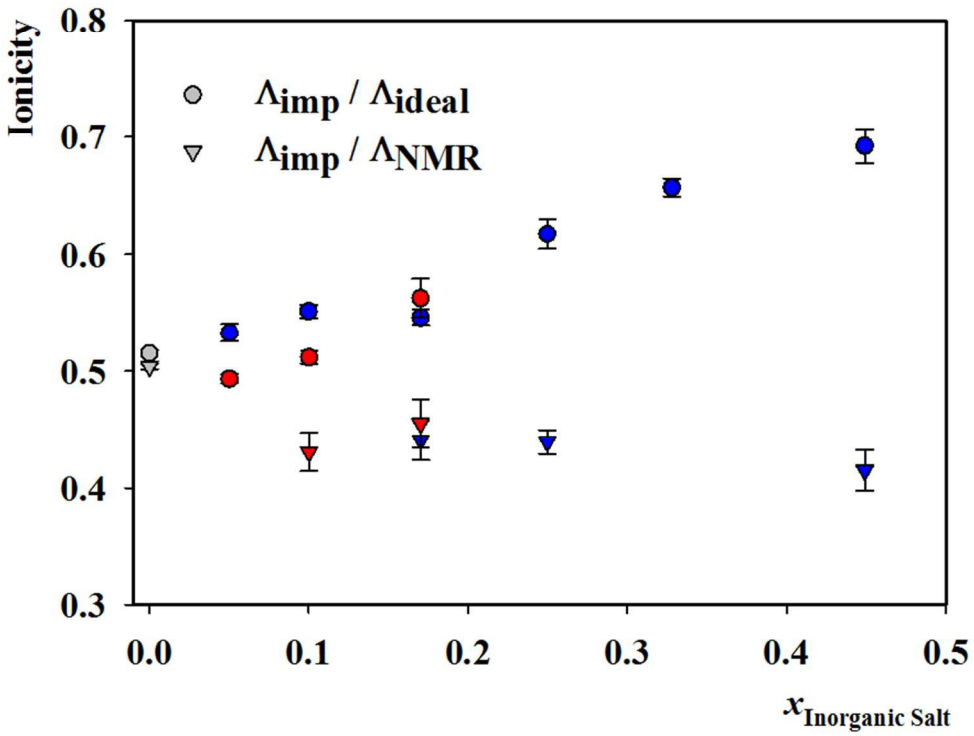

153x124mm (150 x 150 DPI)